IEEE Access
Multidisciplinary | Rapid Review | Open Access Journal

Received April 1, 2019, accepted April 14, 2019, date of publication May 1, 2019, date of current version May 6, 2019.

Digital Object Identifier 10.1109/ACCESS.2019.2912181

Winding Switching and Turn Switching in Permanent Magnet Vernier Machines for Wide Speed Range Operation and High Efficiency

ARSALAN ARIF, NOMAN BALOCH, AND BYUNG-IL KWON, (Senior Member, IEEE)
Department of Electronic Systems Engineering, Hanyang University, Ansan 15588, South Korea

Corresponding author: Byung-il Kwon (bikwon@hanyang.ac.kr)

This work was supported in part by the BK21PLUS Program through the National Research Foundation of Korea within the Ministry of Education, and in part by the National Research Foundation of Korea (NRF) grant funded by the Korea Government (Ministry of Science) (No. NRF-2017R1A2B4007697).

ABSTRACT This paper proposes to turn to switch along with winding switching for high-efficiency of permanent magnet vernier machines (PMVM) during wide speed range operation for electric vehicles application. For winding switching, the three-phase winding of the machine is divided into two sets of windings, namely, winding set A, B, C and winding set X, Y, Z. For turn switching, the number of turns for one set of winding is changed. With the different number of turns for winding set X, Y, Z, the efficiency of the machine can be significantly improved. Initially, the basic electromagnetic characteristics, such as the flux linkage, back electromotive force (EMF), torque, and phase voltages of the machine are investigated using winding switching and turn switching. Then, the output power, torque-speed curve, core losses, efficiency, and power factor of the machine are analyzed in detail using a different number of turns. In addition, the transient effects of winding switching and turn switching have been analyzed. Finally, a control strategy is proposed which combines turn switching and winding switching to ensure high-efficiency of PMVMs during wide speed range operation. A PMVM is designed and driven in accordance with the proposed control strategy (PCS) to show the characteristics of PCS. The PMVM driven with PCS is compared to a recently presented PMVM. The recently presented PMVM is driven by a different control strategy and is analyzed with two different kinds of steel laminations that are general steel (50TW470) and special steel (20JHF1300).

INDEX TERMS High efficiency, permanent magnet vernier machine, turn switching, wide speed range, winding switching.

I. INTRODUCTION

Due to growing concerns on environmental protection, the electric vehicles (EVs) have become a hot research topic and a lot of work has been done regarding advancement of equipment used in EVs [1]–[3]. The permanent magnet vernier machines (PMVMs) are a promising solution for low-speed, direct drive applications such as wind turbine generators, wave energy conversion and EVs [4]. PMVMs produce almost two times back EMF compared to a conventional permanent magnet synchronous machines (PMSMs), hence producing higher torque density. This is owing to their special working principle often called ''magnetic gearing effect'' [5].

The associate editor coordinating the review of this manuscript and approving it for publication was Xiaodong Sun.

Since the inception of PMVMs, many novel topologies have been presented for high torque density [6]–[13].

PMVMs generally have a much higher number of rotor pole pairs compared to stator pole pairs and their operating frequencies are higher compared to general PMSMs. The high operating frequency results in high reactance of the machine leading PMVMs to have a low-power factor [5]. Hence, a high rating inverter is generally required to drive the machine.

Various topologies have been proposed to improve the power factor of PMVMs. Dual-stator spoke-type vernier machines have been presented for high-torque density and high-power factor due to their flux focusing effect [14]–[16]. However, the structure is complicated owing to the presence of two airgaps. The power factor can also be improved by decreasing the armature inductance and this can be achieved

by choosing a proper pole ratio, as discussed in [17]. However, the power factor is still lower than that of the conventional PMSM. Furthermore, increasing the flux linkage can also improve the power factor of a PMVM [18].

In addition, core losses of PMVMs are high due to their high operating frequency. The core loss of a PMVM increases significantly at higher speeds and therefore its efficiency is very low at higher speeds. Owing to these reasons, PMVMs have been generally used for low-speed applications, and their wide speed range analysis is very limited. However, PMVMs have several advantages when used as traction motors. They can be used as a direct-drive in-wheel motor in EVs, hence, achieving the advantages of fast response, gearless operation and zero transmission loss.

In [19], the field winding installed in the armature slots is used to regulate the flux, and the flux modulation teeth are used to produce the vernier effect. However, the extra DC field winding limits the stator fill factor of armature winding and increases the weight of the machine. Moreover, the power factor of the machine is low in the high-speed region. To overcome the above issue of armature fill factor, field winding is installed between the flux modulation teeth to regulate the airgap flux, and consequently use the machine for wide speed range operations [20]. However, the continuous field winding excitation causes additional copper loss. Furthermore, the power factor is low in the high-speed region. The prior publications on wide speed range operation of PMVMs have rarely discussed the efficiency of a vernier machine at wide speed range. In [21], a dual consequent pole vernier memory machine is presented, which uses low coercive force magnets for flux regulation. However, changing the direction of LCF magnets need complex control.

Recently, winding switching has been proposed in PMVMs for wide speed range operation [22]. Using winding switching, the three phases of the machine were divided into two sets of windings: winding set A, B, C and winding set X, Y, Z. The turns of the two sets of windings were equal. The current in the two sets of winding was additive initially and the mode of operation was called cumulative mode. The current in the winding set X, Y, Z was reversed in the differential mode for wide range operation. However, there were some shortcomings in [22], that are, efficiency of the machine was low during wide speed range operation and torque of the machine was low in differential mode. In order to compensate the low torque, the armature current was increased in differential mode, hence, current density of the machine was increased.

This study proposes turn switching and winding switching to achieve high efficiency during wide speed range operation of PMVMs for EV application. The proposed technique solves the above mentioned problems of [22]. In turn switching, the number of turns of the windings set X, Y, Z are changed using switches. By using different number of turns, the efficiency of the machine during wide speed range is improved. Also, the current density of the machine remains same throughout wide speed range operation. A detailed analysis is performed with different number of turns of X, Y, Z set

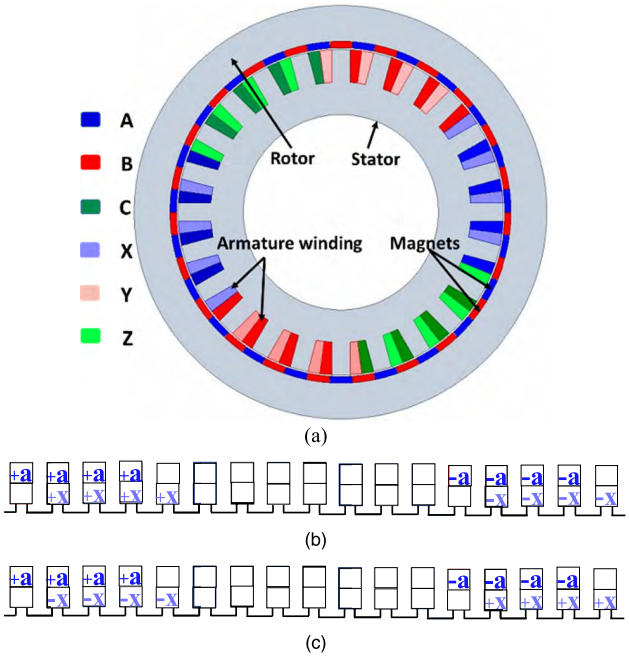

FIGURE 1. Topology and operating modes of PMVM. (a) Topology. (b) Cumulative mode. (c) Differential mode.

of winding that is 10, 20, and 35, respectively. Torque-speed and efficiency-speed curves are obtained for each number of turns and meaningful conclusions are drawn at the end of the paper. Furthermore, a control strategy is proposed, which combines winding switching and turn switching for high efficiency during wide speed range operation. The operation of PMVM using winding switching [22] is analyzed with two types of materials namely, general steel (50TW470) and special steel (20JNHF1300). Finally, the proposed control strategy (PCS) is compared to [22] to show its effectiveness. The advantages and limitations of each method are also elaborated at the end of this paper.

II. TOPOLOGY AND WORKING PRINCIPLE WITH WINDING SWITCHING AND TURN SWITCHING

A. TOPOLOGY

An outer rotor PMVM is designed to show its wide speed range characteristics using winding switching, as shown in Fig. 1(a). The outer rotor topology can be directly coupled with the wheel of an EV resulting in a direct-drive machine for EV application. The main parameters of the machine are shown in Table 1. The designed PMVM has a 24-slot stator, 2 pole stator armature winding and a 46-pole outer PM rotor. The three-phase armature winding of PMVM has been divided into two sets of windings as shown in Fig. 1(b). The two sets of windings A, B, C, and winding X, Y, Z, are placed such that they are one slot apart, and hence, they yield a phase shift of $\pi/12$ radians with respect to each other.

B. WORKING PRINCIPLE

A PMVM has a higher number of rotor pole pairs compared to stator pole pairs and operates based on the so called

TABLE 1. Main parameters of PMVM.

Item	Unit	Value
Rotor outer diameter	mm	254
Rotor inner diameter	mm	202
Stator outer diameter	mm	200
Stator inner diameter	mm	120
Stack length	mm	70
Rated speed	rpm	300
Rated torque	Nm	17.18
Rated Current	A	1.5
Rated Power	W	539.7
Rated Voltage	V	246.4
Rotor PM pole pairs	-	23
Stator slots	-	24
Turns/phase	-	280
Armature pole pairs	-	1
Airgap length	mm	1

"magnetic gearing effect". In PMVMs, a small movement of rotor produces a considerable change in the flux, thus producing higher back EMF compared to a conventional PMSM. In order to produce the magnetic gearing effect, a PMVM must satisfy (1).

$$Z_r = Z_s - P \tag{1}$$

where Z_r is number of rotor pole pairs, Z_s is the number of stator slots and P is the number of armature pole pairs, respectively. For this paper, Z_r, Z_s, and P, are chosen to be 23, 24, and 1, respectively. Although, many combinations of Z_r, Z_s, and P can satisfy (1), the above combination enables maximum flux weakening range [23]. Therefore, using the above combination of Z_r, Z_s, and P, maximum advantage of winding switching is utilized in vernier machines.

Even though, the rotor and stator pole pairs are different, the machine achieves a smooth torque by synchronizing the space harmonics of the rotor MMF with the stator MMF. The flux from the rotor PMs is modulated by the open stator teeth and produces a component that is equal to stator pole pairs in the airgap flux density. This component interacts with the stator MMF to produce steady torque.

The airgap flux density of the machine is shown in Fig. 2(a), whereas its harmonic spectra is shown in Fig. 2(b). It can be observed that the airgap has two major components that is 23rd pole pair component and the modulated 1st pole pair component. These two components are the working harmonics and are coupled with the corresponding harmonics of stator MMF to produce steady torque. Moreover, it should be noted the proposed machine uses ferrite magnets to maintain a low machine cost.

Based on winding switching, PMVM operates in two modes, namely cumulative and differential mode. In the cumulative mode, the polarity of the two sets of windings (A, B, C, and X, Y, Z) is the same as shown in Fig. 1(b). The fluxes from the two sets of windings add up and generate the maximum torque that the machine can produce in a normal three-phase machine configuration. To use the machine for

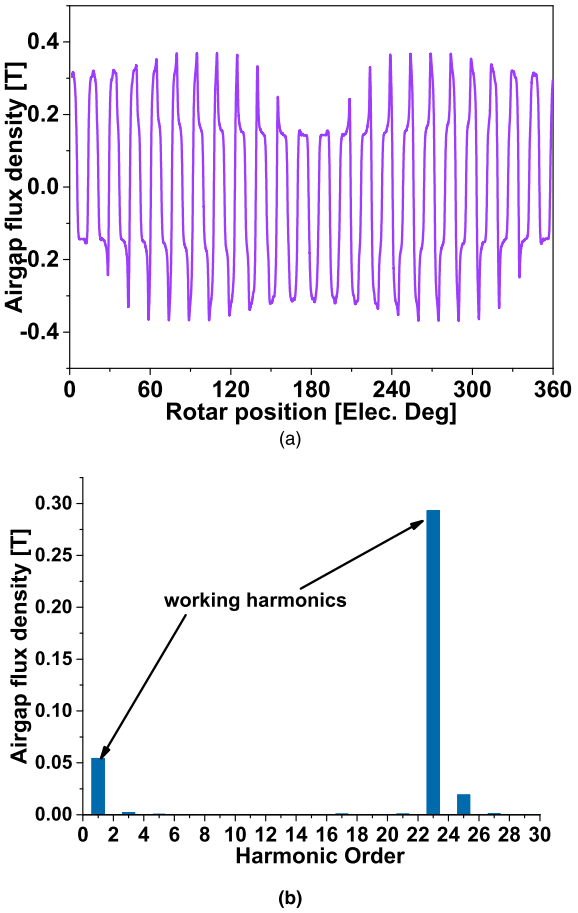

FIGURE 2. Airgap flux density. (a) Waveform. (b) Harmonic order.

wide speed range operation, the polarity of the X, Y, Z set of winding is reversed, as shown in Fig. 1(c), which is the differential mode operation. In the differential mode, the flux from winding set X, Y, Z is subtracted from winding set A, B, C and therefore, the total flux is reduced. In differential mode, due to the subtractive effect of the flux, both the inductance and back EMF of the machine are decreased.

The phase voltages of a dual three phase machine for A and X phases are given by (2) and (3), respectively [20].

$$V_{as} = i_{as}r_s + L_{as}\frac{di_{as}}{dt} + \frac{1}{\sqrt{2}}(L_m + l_m)\frac{di_{xs}}{dt} - \frac{1+\sqrt{3}}{2\sqrt{2}}(L_m + l_m) \times \frac{di_{ys}}{dt} + \frac{-1+\sqrt{3}}{2\sqrt{2}}(L_m + l_m)\frac{di_{zs}}{dt} + \lambda_m\omega_e \cos(\omega_e t) \tag{2}$$

$$V_{xs} = i_{xs}r_s + L_{xs}\frac{di_{as}}{dt} + \frac{1}{\sqrt{2}}(L_m + l_m)\frac{di_{as}}{dt} + \frac{-1+\sqrt{3}}{2\sqrt{2}}(L_m + l_m) \times \frac{di_{bs}}{dt} - \frac{1+\sqrt{3}}{2\sqrt{2}}(L_m + l_m)\frac{di_{cs}}{dt} + \lambda_m\omega_e \cos(\omega_e t - \pi/12) \tag{3}$$

The ABC and XYZ variables of the machine windings are transformed into stationary frame components q_1^s, d_1^s, q_2^s and

d_2^s using (4) and (5), respectively.

$$\begin{bmatrix} V_{q1}^s \\ V_{d1}^s \\ V_{01}^s \end{bmatrix} = \frac{3}{2} \begin{bmatrix} 1 & -\frac{1}{2} & -\frac{1}{2} \\ 0 & -\frac{\sqrt{3}}{2} & \frac{\sqrt{3}}{2} \\ \frac{1}{2} & \frac{1}{2} & \frac{1}{2} \end{bmatrix} \begin{bmatrix} V_{as} \\ V_{bs} \\ V_{cs} \end{bmatrix} \tag{4}$$

$$\begin{bmatrix} V_{q2}^s \\ V_{d2}^s \\ V_{02}^s \end{bmatrix} = \frac{3}{2} \begin{bmatrix} \frac{1}{\sqrt{2}} & -\frac{1+\sqrt{3}}{2\sqrt{2}} & \frac{-1+\sqrt{3}}{2\sqrt{2}} \\ -\frac{1}{\sqrt{2}} & \frac{-1+\sqrt{3}}{2\sqrt{2}} & \frac{-1+\sqrt{3}}{2\sqrt{2}} \\ \frac{1}{2} & \frac{1}{2} & \frac{1}{2} \end{bmatrix} \begin{bmatrix} V_{xs} \\ V_{ys} \\ V_{zs} \end{bmatrix} \tag{5}$$

These stationary frame of reference equations can be transformed into a synchronous frame of reference using (6)

$$\begin{bmatrix} V_{q1}^e \\ V_{d1}^e \\ V_{q2}^e \\ V_{d2}^e \end{bmatrix} = \begin{bmatrix} \cos(\theta_e) & -\sin(\theta_e) & 0 & 0 \\ \sin(\theta_e) & \cos(\theta_e) & 0 & 0 \\ 0 & 0 & \cos(\theta_e) & -\sin(\theta_e) \\ 0 & 0 & \sin(\theta_e) & \cos(\theta_e) \end{bmatrix} \begin{bmatrix} V_{q1}^s \\ V_{d1}^s \\ V_{q2}^s \\ V_{d2}^s \end{bmatrix} \tag{6}$$

where V_{as} and V_{xs} are the voltages of phase A and phase X, i_{as}, i_{bs}, i_{cs}, i_{xs}, i_{ys} and i_{zs} are the currents in Phase A, B, C, X, Y and Z, respectively. L_{as} and L_{xs} are the self-inductances of phase A and phase X, ω_e is electrical angular velocity, r_s is stator resistance, λ_m is flux linkage due to permanent magnets, L_m is magnetizing inductance and l_m is leakage inductance of the mutual component between two three-phase windings, respectively.

The 1st term on the right hand side of (2) shows the resistive voltage drop, whereas, 2nd, 3rd, and 4th term show the inductive voltage drop considering the mutual inductances between phases, and the last term shows the back EMF. In PMVM, the back EMF and the inductive voltage drop have a major portion in the phase voltages which limits its application for wide speed range operation. The inverter limit is generally assumed to be the phases voltages of the machine obtained at the rated speed. The phase voltages should not increase beyond the rated voltages of the inverter at any speed. To use PMVM for wide speed range operation, the machine is switched from the cumulative mode to the differential mode. This results in lower inductive voltage drop and back EMF, and consequently, the phase voltages of the machine are reduced. Therefore, the speed of the machine can be increased.

Moreover, the flux from the two sets of windings is additive during operation in the cumulative mode and subtractive during operation in the differential mode, as shown in Fig. 3(a) and Fig. 3(b), respectively. In cumulative mode, the currents enter at the dotted end of both windings to generate positive MMF in both sets of windings. There is a common neutral connection using thyristors at the center of two windings. Therefore, the net MMF is the sum of MMF from two windings. In differential mode as shown in Fig. 3(b), the thyristors are turned off such that now currents enter at the dotted end of A, B, C winding and leave at the dotted end of X, Y, Z winding. Since, the direction of X, Y, Z set of winding is reversed, winding A, B, C produces a positive MMF, whereas, winding set X, Y, Z produces a negative MMF. In this case, the net MMF is the difference of MMFs in two windings. Furthermore, as it can be observed in Fig. 3(a), different switches have been installed across the winding set X, Y, Z. In normal operation, the switches are off, and hence the machine utilizes the complete turns of the winding set X, Y, Z. However, when the switch S_1 is turned on, only 10 turns of the winding set X, Y, Z, will be utilized. Similarly, when the switch S_2 is turned on, 20 turns of the winding set X, Y, Z, will be utilized. The advantages and disadvantages for using different number of turns for the winding set X, Y, Z, will be elaborated in the coming sections. The different number of turns of two sets of windings have been named differently as shown in Table 2.

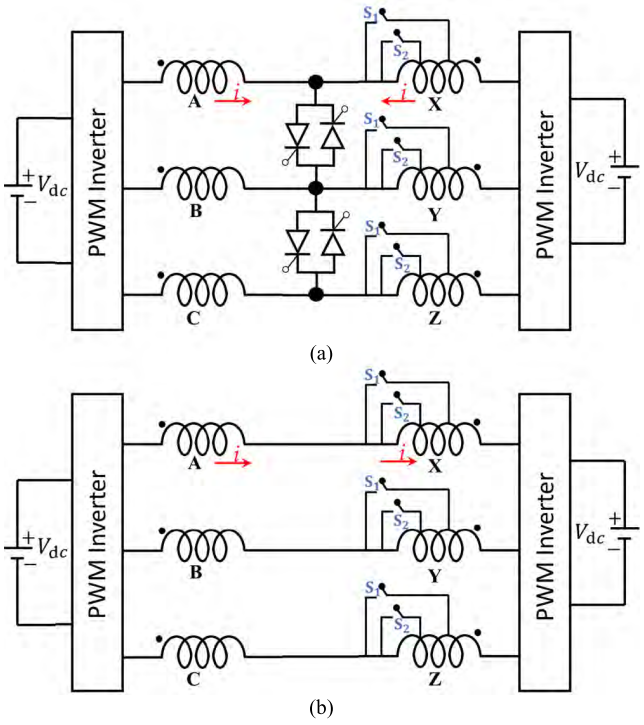

FIGURE 3. Machine modes with switches. (a) Cumulative mode. (b) Differential mode.

III. PERFORMANCE ANALYSIS OF PMVM IN DIFFERENT CONDITIONS

The base speed of the machine is 300 rpm. If the base speed is chosen high, the efficiency of the machine below base speed is low. Choosing low base speed provides high efficiency even

TABLE 2. Different conditions for winding switching in cumulative and differential mode.

Condition		Con1	Con2	Con3(Winding Switching only)
Turns of Winding Set X, Y, Z/Slot		10	20	35
Turns of Winding Set A, B, C/Slot		35	35	35
Resistance (Ω)	Phase A	1.21	1.21	1.21
	Phase X	0.35	0.7	1.21
	Total Equivalent Resistance in Cumulative Mode	0.27	0.44	0.6
	Total Equivalent Resistance in Differential Mode	1.56	1.91	2.42

during very low speed operations. Also, the maximum speed of the machine is very high using winding switching [22], hence, low base speed is a preferable choice keeping in mind the direct drive application of proposed machine. Initially, the finite element method (FEM) analysis results pertaining to the cumulative and differential mode of the machine are analyzed at this speed with different number of turns. FEM has been performed using the commercial software "Ansys Maxwell version 19". The quality of the mesh was kept good; the number of the elements of the mesh were kept high for the stator, rotor, band and region. Due to high quality of mesh, each simulation took around 45 minutes.

The comparison of flux linkage of the machine at 300 rpm during operation in the cumulative and differential mode for Con1, Con2 and Con3 is shown in Fig. 4(a) and Fig. 4(b), respectively. In the cumulative mode, the flux linkage is the lowest for Con1, followed by Con2, the highest flux linkage is for Con3. This is owing to higher effective turns/phase in Con3 than the other two conditions. In the differential mode, the flux linkage is lowest for Con3. This is because, the maximum flux is subtracted between the two sets of windings in this condition.

The comparison of the back EMFs of the machine in the cumulative and differential modes for all three conditions is shown in Fig. 5(a) and Fig. 5(b), respectively. In cumulative mode, back EMF is the lowest in Con1, followed by Con2, while the largest back EMF is obtained in Con3. In the differential mode, the back EMF obtained in Con1, Con2, and Con3 is 43.82 V, 29.03 V and 13.37 V, respectively. The ratio of back EMF obtained in cumulative mode to the back EMF obtained in differential mode is the flux weakening obtained for each condition and is expressed by (7)

$$F_W = E_{cum}/E_{diff} \tag{7}$$

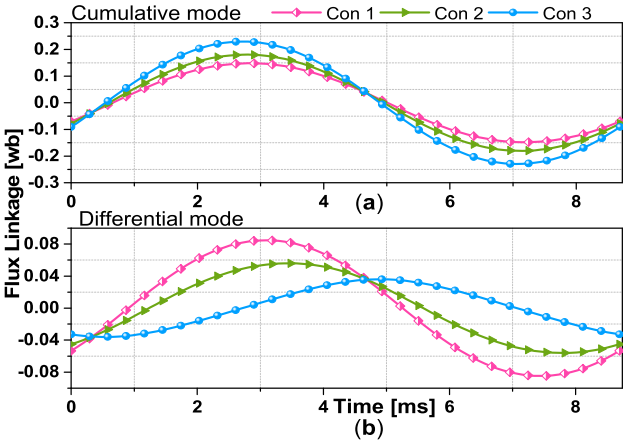

FIGURE 4. Comparison of flux linkage. (a) Cumulative mode. (b) Differential mode.

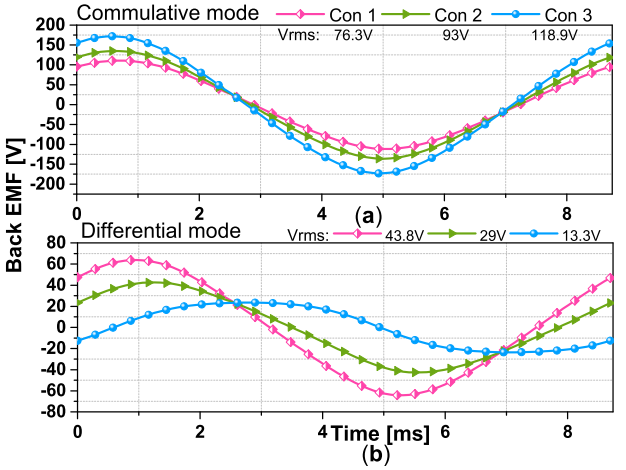

FIGURE 5. Comparison of back EMF. (a) Cumulative mode. (b) Differential mode.

For Con1, Con2, and Con3, these ratios are found to be 1.74, 3.2 and 8.89, respectively. Hence, flux weakening obtained only due to back EMF drop in differential mode in Con1, Con2, and Con3 are 1.74, 3.2 and 8.89 times, respectively.

A. INDUCTANCE AND POWER FACTOR

The self-inductance of one phase of the PMVM with different turns in cumulative and differential mode is shown in Fig. 6(a) and Fig. 6(b), respectively. In the cumulative mode, Con1 has the lowest inductance, followed by Con2, whereas, Con3 has the highest inductance. This is because, the effective number of turns of Con1 are the lowest, whereas, Con3 has the highest number of turns.

It should be noted that the mutual inductances also influence the output torque and phase voltages of the machine in the load condition. The mutual inductances have an additive effect on the net inductance in cumulative mode and a subtractive effect in differential mode. The mutual inductance depends on the angle between two sets of windings. However, the back EMF is not affected due to mutual inductances.

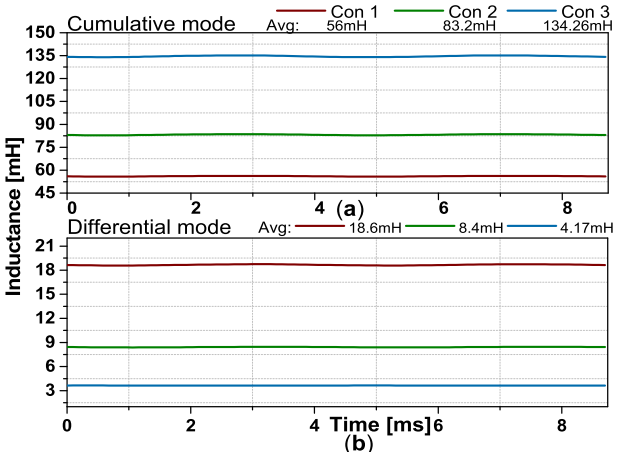

FIGURE 6. Comparison of inductance. (a) Cumulative mode. (b) Differential mode.

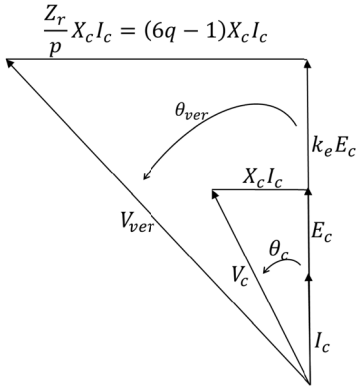

FIGURE 7. Phasor diagram of PMVM.

This is because back EMF is taken in no load condition and therefore no current flows in either set of winding in this condition, which results in zero mutual inductance between the phases.

If the resistive voltage drop is ignored, the phasor diagram of a vernier machine in comparison to a conventional PMSM is shown in Fig. 7, whereby the power factor of the vernier machine is given by (8) [2].

$$\cos\theta_{ver} = \frac{1}{\sqrt{1 + (\frac{Z_r}{pk_e})^2 tan^2\theta_c}} \tag{8}$$

where k_e is the coefficient of the voltage boost in the vernier machine, E_c is the back EMF, X_c is the reactance, θ_{ver} and θ_c are the power angles, respectively. The power factor depends on θ_c, which in turn depends on the reactance of the machine. The reactance depends on the frequency and inductance of the machine. The designed PMVM has high number of rotor pole pairs and a low number of stator pole pairs, hence, its frequency and inductance are both high. Consequently, the reactance of the machine is high, and the power factor is low. The power factor of the machine in the cumulative

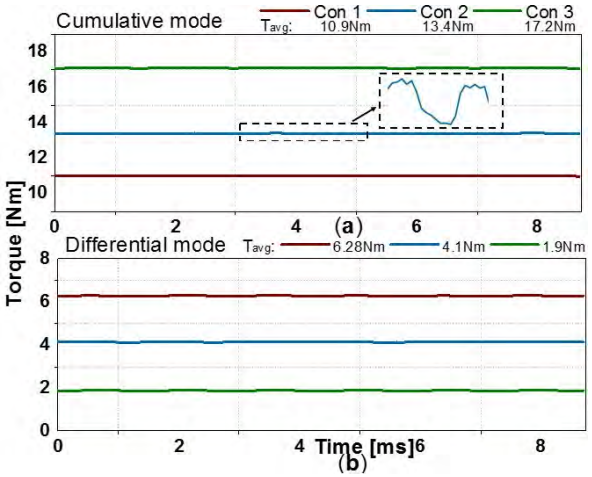

FIGURE 8. Comparison of torques. (a) Cumulative mode. (b) Differential mode.

mode for Con1, Con2, and Con3 are 0.66,0.6, and 0.51, respectively.

However, when the machine is switched to the differential mode, the inductance of the machine is significantly decreased. This is because the flux from the two sets of windings is subtracted and consequently, the effective number of turns is reduced. Inductance is decreased 3 times in Con1, 9.9 times in Con2 and 32 times in Con3. In Con3 (cumulative mode), power factor was lowest. However, in Con3 (differential mode), power factor is highest. This is due to lowest inductance of Con3 in differential mode. Also, due to lowest, inductance in differential mode of Con3, phase voltages will drop considerably, thus enabling maximum wide speed range operation. The power factor of the machine in differential mode for Con1, Con2, and Con3 are 0.83, 0.9, and 0.96, respectively.

B. TORQUE AND PHASE VOLTAGES

The torque of the PMVM in cumulative and differential mode in Con1, Con2 and Con3 is shown in Fig. 8(a) and Fig. 8(b), respectively. In the cumulative mode, Con3 has the highest torque. The torque ripple of the machine is low in all conditions (less than 5%). The low-torque ripple is an inherent characteristic of PMVMs. Moreover, in the differential mode, Con3 has the lowest torque. Even though, large torque is an advantage of Con3 in cumulative mode, very low torque in the differential mode is a drawback of this condition. Due to low torque, the power of the machine is dropped significantly in differential mode. This low torque becomes a hurdle in wide speed range operation which is discussed in a subsequent section. Large torque in the differential mode is an advantage for Con1, which results in high efficiency during wide speed range operation. This is explained in more detail in the upcoming section.

The phase voltages of the machine in cumulative and differential modes of operation in different conditions are shown in Fig. 9(a) and Fig. 9(b), respectively. In the cumulative

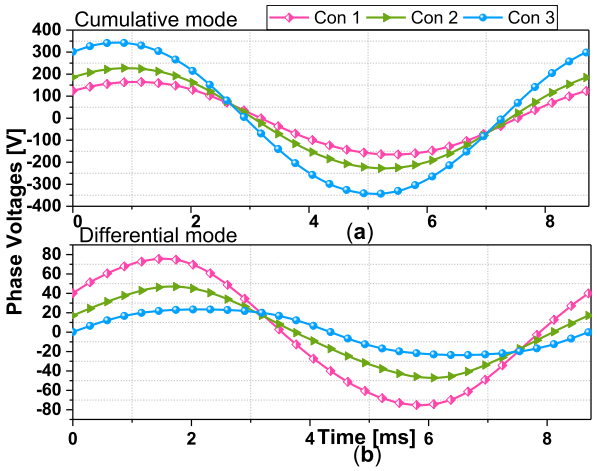

FIGURE 9. Comparison of phase voltages. (a) Cumulative mode. (b) Differential mode.

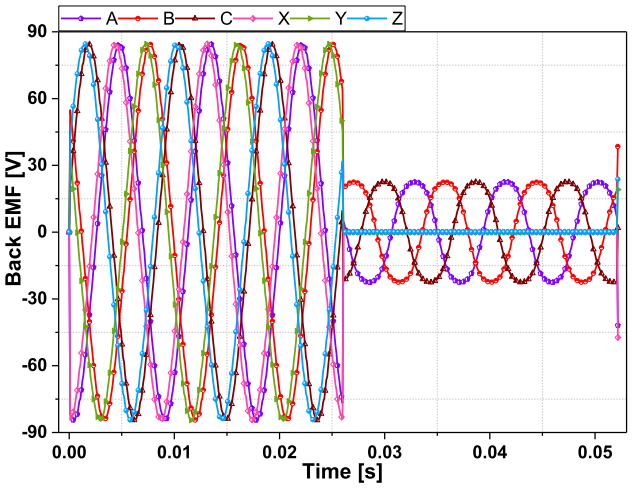

FIGURE 10. Back EMF in two modes (Transient analysis).

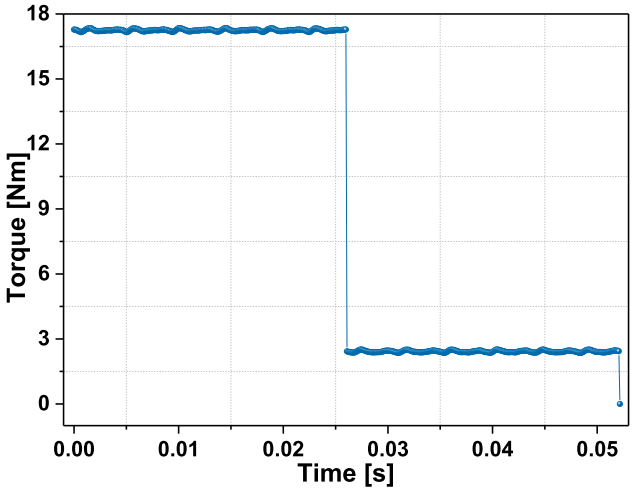

FIGURE 11. Torque in two modes (Transient analysis).

TABLE 3. Overall comparison in different conditions.

Parameter	Con1	Con2	Con3 (Winding switching only)
	Cumulative/ Differential	Cumulative/ Differential	Cumulative/ Differential
Back EMF (V)	76.37/43.82	93.1/29.03	118.9/13.37
Torque (Nm)	10.9/6.28	13.4/4.15	17.18/1.90
Inductance (mH)	56.07/18.6	83.2/8.4	134.26/4.17
Phase voltages (V)	118.47/53.2	163.4/32.09	246.4/14.2
Power factor	0.66/0.83	0.6/0.9	0.51/0.96

mode, Con3 has the highest phase voltages owing to its higher back EMF and higher inductance.

In the differential mode, Con3 has the lowest phase voltages compared to all other conditions. This is because, its effective flux is reduced much more than other conditions. The lower phase voltages provide Con3 maximum advantage of wide speed range operation. Hence, by comparing the phase voltages of the machine in the two modes, it can be said that the variable speed range of Con1 is the minimum, followed by Con2, whereas Con3 has the maximum variable speed range. The comparison of the machine performance in different conditions is listed in Table 3.

C. TRANSIENT ANALYSIS IN DIFFERENT CONDITIONS

As the proposed machine needs to switch to different conditions in cumulative as well as differential mode for high efficiency and wide speed range operation using switches, therefore, it is important to analyze the effect of transients at the instant of switching from one mode to another. In order to analyze the effect of switching on inverter, transient simulations were performed, which were similar to the experiment. Fig. 10 shows the back EMF of the proposed machine when it switches from cumulative mode to differential mode. The simulation was performed for 6 electrical cycles. The machine runs in cumulative mode for the first 3 cycles and the last 3 cycles, the machine is switched to differential mode. The decrease in back EMF shows that the machine can be switched from cumulative mode to differential in running condition. Fig. 11 shows the torque of the machine from cumulative mode to differential mode. It can be observed that torque is high in cumulative mode and it drops as soon as the machine is switched to differential mode. All the simulation results shown in this paper have been performed using current source. The transient simulations were also performed using current source. Therefore, the effect of switching was visible in phase voltages. Fig. 12 shows the effect of switching on

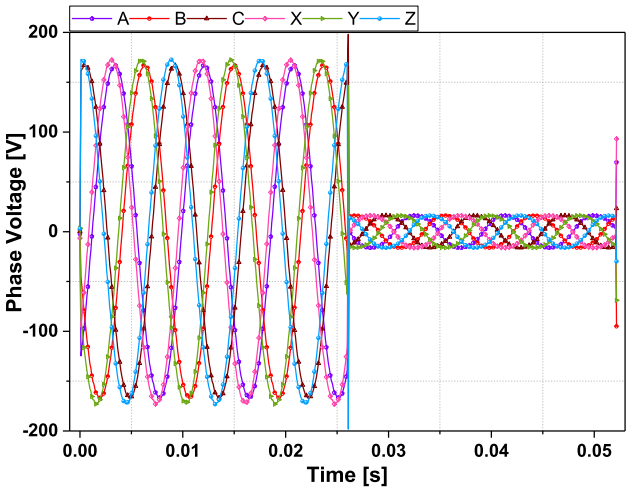

FIGURE 12. Phase voltages in two modes (Transient analysis).

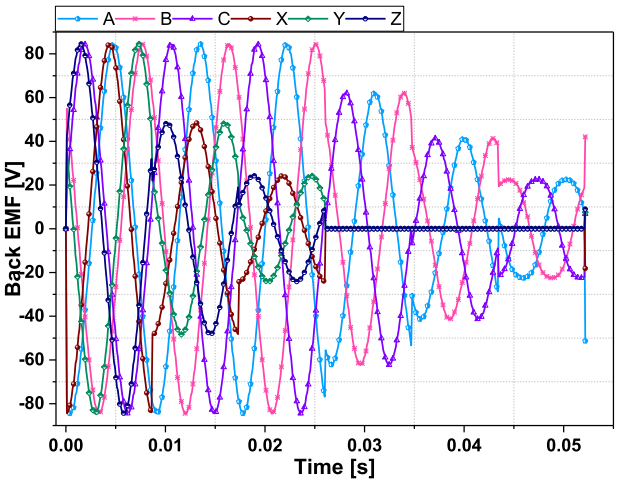

FIGURE 13. Back EMF in all conditions (Transient analysis).

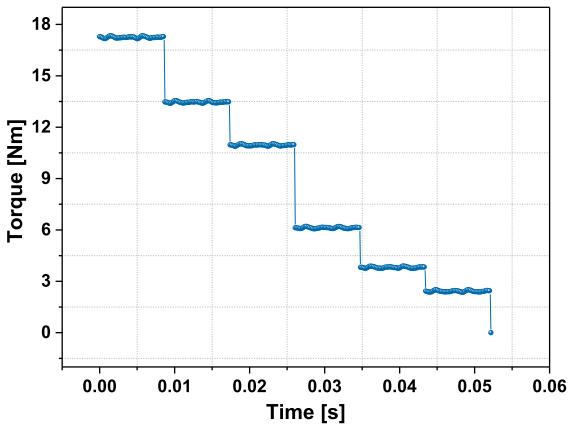

FIGURE 14. Torque in all conditions (Transient analysis).

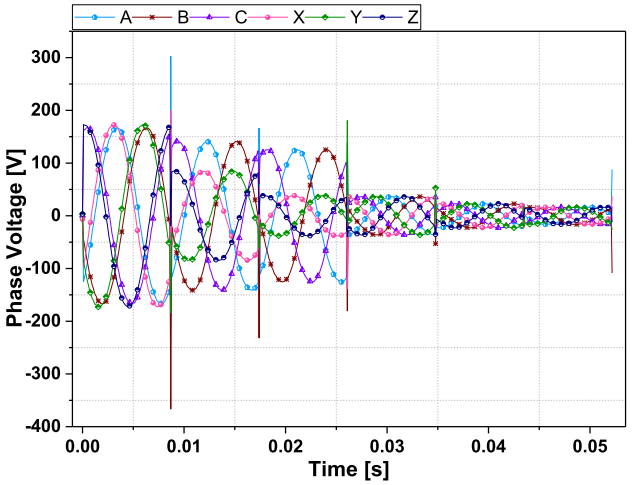

FIGURE 15. Phase Voltages in all conditions (Transient analysis).

phase voltages, where the machine is being switched from cumulative mode to differential mode. It can be observed that at the switching instant, the peak phase voltages are increased from 168 V to 200 V, which is about 19%. Moreover, the transient period is very small (about a millisecond). Hence, it can be said that switching will not damage or trip the inverter.

Also, the machine switches to different conditions (Con1, Con2, Con3) in both cumulative and differential mode. Fig. 13 shows the back EMF of the machine, while the machine is switched in different conditions. The machine is simulated for 6 electrical cycles. In the first electrical cycle, the machine is running in cumulative mode Con3. Both phase A, B, C and X, Y, Z provide maximum back EMF, which is added in cumulative mode. In the 2nd cycle, the machine is switched to Cumulative mode con2, here the back EMF of phase X is decreased where phase A remains the same. In the 3rd cycle, the machine is switched to cumulative mode con3, here, back EMF of phase X is further decreased whereas phase A remains the same. The machine is then switched to differential mode Con1. After the 3rd cycle, both phase A and X (A + X) are shown. This is due to the limitation of the simulation which could only show the combine effect in the circuit rather than individual back EMFs. In the 4th, 5th and 6th cycle, the machine runs in differential mode Con1, differential mode Con2 and differential mode Con3, respectively. It can be observed that the machine can be smoothly switched in different conditions and the back EMF of the machine is decreased, consequently, speed of the machine can be increased. The torque of the machine while switching to different conditions is shown in Fig. 14. It can be observed that after each cycle, torque of the machine is decreased. This is because, back EMF decreases after each condition. The advantages of each condition are elaborated in the next section. The phase voltages of the machine in all conditions are shown in Fig. 15. It can be observed that at switching instant, the phase voltages of the machine are increased for a brief period. The peak phase voltages reach up to 300 V when the machine is switched from cumulative mode Con3 to cumulative Con2, this is the maximum switching transient.

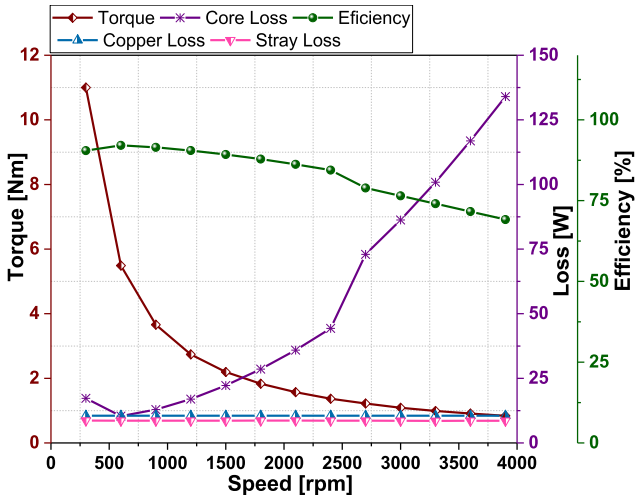

FIGURE 16. Torque-speed curve and efficiency in condition 1 (Con1).

This increase is around 78.5%. However, the switching transient is for a very brief period (around one millisecond). Hence, it can be said that the switching period will not damage or trip the inverters. Moreover, capacitors can be installed around switches which will limit the phase voltages at the instant of switching. The transient analysis of the proposed machine shows that the machine can be switched to different conditions in running condition, which will not damage or trip the inverter due to switching transients.

IV. WIDE SPEED RANGE ANALYSIS

Detailed FEM simulations were performed to explore the variable speed characteristics of PMVM using winding and turn switching. Three conditions were chosen for turn switching. Each condition has different number of turns and these conditions represent different speed regions of the machine. In cumulative mode, Con3 uses the maximum turns and therefore, it provides maximum torque and maximum power. This condition is required at low speed. Hence, Con3 basically represents low speed region. Con2, uses less turns and therefore, its torque and power are lower compared to Con1. However, its efficiency is high owing to lower core losses. As we move towards high speed region, we require lower torque. However, core losses of the machine start to become significant, which decreases the efficiency of the machine. We use Con2 during medium speed region and hence, Con2 represents the medium speed region. Con3, uses the minimum number of turns among all conditions. Its torque and power are lowest among all conditions. Also, its core and copper losses are lower compared to other two conditions (Con2 and Con3). Low torque and lower losses are most beneficial at high speed region. Hence, Con3 represents high speed region.

A. WIDE SPEED RANGE ANALYSIS FOR CON1, CON2 AND CON3

In Con1, the total turns per slot for X, Y, Z set of winding is 10 whereas it is 35 for A, B, C set of winding. Since, the total turns/slot of this condition are smaller than all other conditions. Therefore, its torque and power are also smaller than other conditions. The torque speed curve and efficiency speed curve of the machine during wide speed range operation for Con1 are shown in Fig. 16. Throughout the entire wide speed range of operation, the power of the machine remains constant. However, to maintain constant power, the torque of the machine is decreased with increasing speed. In this paper, efficiency (η) is calculated using (9)

$$\eta = \frac{P_{out}}{P_{out} + P_{cu} + P_{iron} + P_{s+m}} \times 100 \tag{9}$$

where P_{out}, P_{cu}, P_{iron} and P_{s+m} represents the output power, copper losses, iron losses, and stray and mechanical losses, respectively. The copper losses are calculated by estimating the resistance of the winding per phase and armature currents, whereas, the iron losses are calculated using FEM. The FEM considers hysteresis loss, eddy current loss and added loss in calculation of core losses similar to [24]. The stray and machinal losses are assumed to be 2.5% of the output power. Ferrite magnets have been used throughout the analysis in this paper. The PM eddy current losses were found to be very low due to high resistance of ferrite PMs and therefore, these losses were ignored in efficiency calculation.

The torque speed curve of the machine in Con1 is shown in Fig. 16. From 0–300 rpm, the machine is operated in the cumulative mode. From 300–2700 rpm, the torque and phase voltages of the machine are decreased using negative d-axis while remaining in the cumulative mode. At 2700 rpm, the inverter limit is reached, and the machine is switched to differential mode. The phase voltages and torque of the machine are decreased in this mode. Note that as soon as the machine is switched to differential mode, the negative d-axis is released (id = 0). This is because the phase voltages are decreased already due to switching the machine in differential mode. At 2700 rpm, the required torque to maintain constant power is 1.22 Nm whereas, the torque generated in the differential mode is 6.28 Nm. Hence, the obtained torque in the differential mode is still larger than the torque required for maintaining constant power. Therefore, the negative d-axis current which was previously turned zero at point of winding switching, is applied again in the differential mode to decrease the torque. By applying d-axis current, the q-axis component of the current is decreased, which decreases the torque of the machine to maintain constant power.

The iron loss, copper loss and efficiency curve of the machine during wide speed range operation in Con1 is shown in Fig. 16. The iron losses tend to increase with increasing speed of the machine which is due to increasing frequency. However, the copper losses are low and remain almost same throughout the wide speed range. That's because the armature current has not been increased beyond the rated point anywhere during the entire wide speed range. The efficiency of the machine at base speed is high. With increasing speed, the efficiency is decreased gradually due to higher core losses of the machine. The minimum efficiency at the highest speed

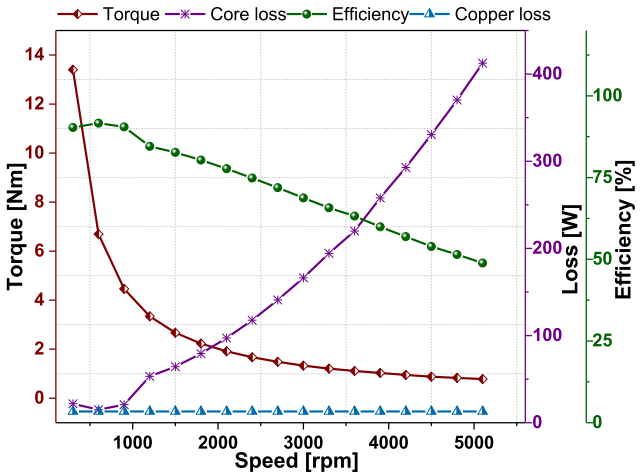

FIGURE 17. Torque-speed curve and efficiency in condition 2 (Con2).

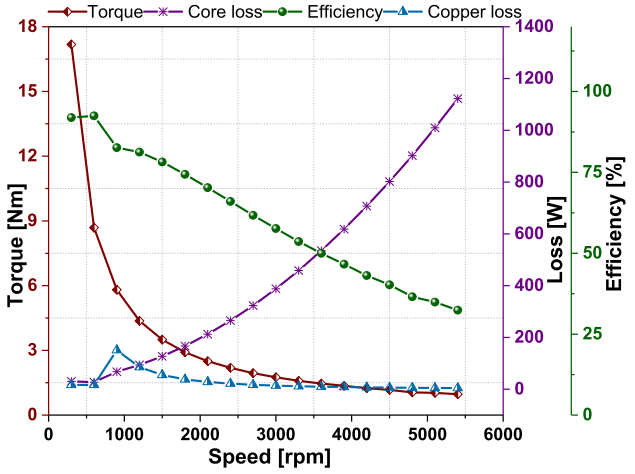

FIGURE 18. Torque-speed curve and efficiency in condition 3 (Con3).

(3900 rpm) of the machine is 70%. Hence, this condition provides good efficiency during the entire wide speed range operation.

The losses, efficiency and torque speed curve for Con2 and Con3 are shown in Fig. 17 and Fig. 18, respectively. It can be observed that Con2 and Con3 have higher maximum speed limit compared to Con1, however, the efficiency of the machine is comparatively low. The comparison has been explained in detail in the next section.

B. COMPARISON OF WIDE SPEED RANGE ANALYSIS IN DIFFERENT CONDITIONS

The comparison of the torque speed curve and efficiency of all conditions over wide speed range operation is shown in Fig. 19. In Con1, the torque is lowest, however, the efficiency is the highest. The maximum speed range is also limited to 3900 rpm in this condition. This is because the winding set X, Y, Z, has less turns, and the difference of the back EMF and torque between the cumulative and differential modes

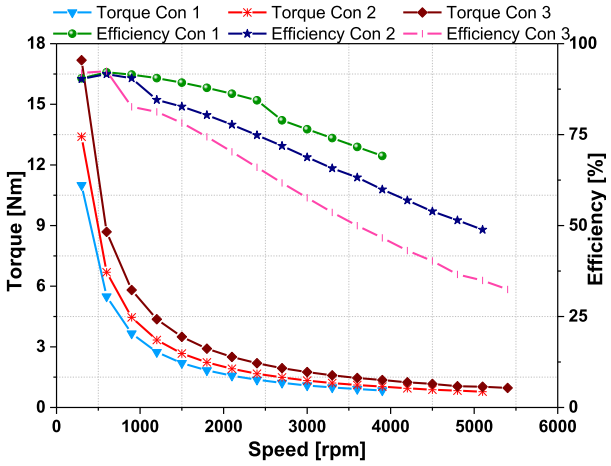

FIGURE 19. Comparison of all torque speed curves and efficiencies.

is not high. The lower difference of the torque observed in the differential mode is an advantage. Hence, the negative d-axis current is also used in the differential mode. Therefore, the core losses are limited, which results in a good efficiency throughout the wide speed range.

In Con2, the torque is higher than that in Con1. Furthermore, the maximum speed of the machine is 5100 rpm, which is greater than that in Con1. However, in this mode of operation, due to increased number of turns, the core losses are higher, and the efficiency of the machine is lower compared to Con1.

In Con3, the speed range of the machine is increased to 5400 rpm, that is greater than Con1 and Con2. However, efficiency of the machine is lowest in this mode. An important issue faced is that when the machine is switched to differential mode at 600 rpm, the required torque to maintain constant power is much larger than the torque available in differential mode. Therefore, the armature current is increased to maintain constant power. Hence, the current density of the machine is also increased.

V. PROPOSED CONTROL STRATEGY (MERITS AND LIMITATIONS)

The efficiency of the vernier machine in wide speed range operation is low utilizing only winding switching. Therefore, for high efficiency of PMVMs during wide speed range operation, the control strategy as shown in Fig. 20 is proposed.

In proposed control strategy (PCS), initially, the machine will be started with both switches turned off and hence the machine will start in Con3 (cumulative mode) with its maximum power capacity. The machine will remain in this mode from zero rpm to the base speed of 300 rpm. Therefore, the maximum possible torque and efficiency will be obtained. Then switch S_2 will be turned on. The machine will switch to cumulative mode Con2. The machine will remain in cumulative mode of Con2 till its maximum limit of 900 rpm. Here, power is dropped a little, however, advantages are

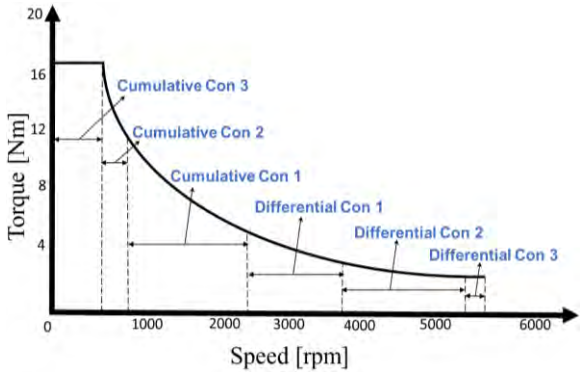

FIGURE 20. Proposed control strategy.

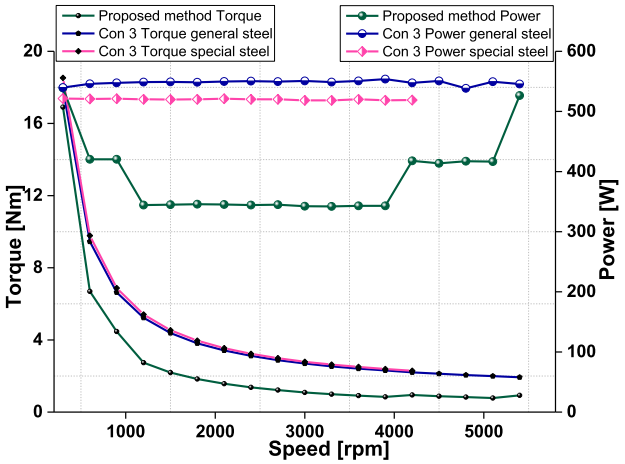

FIGURE 21. Comparison of the proposed control strategy with con3 (general and special steel).

better efficiency. Then switch S_1 will be turned on, hence, the machine will be switched to Con1 in cumulative mode. The machine remains in this mode until its maximum speed limit is reached. At 2700 rpm, the machine is switched to the differential mode of Con1. This mode will remain in effect, until the maximum speed of this condition is reached, that is 3900 rpm. Until this point the machine will be running in its highest possible efficiency mode. When the maximum speed of this condition is achieved, the switch S_2 will be turned on, and the switched S_1 will be turned off. From 3900 rpm to 5100 rpm, the machine will remain in differential mode. Finally, both switches S_1 and S_2 will be turned off (Con3 differential) and the machine will utilize all its turns. In this mode, the machine will provide the maximum wide speed range.

Moreover, from 5100 rpm to 5400 rpm, the required torque of the machine is very low to maintain constant power. Hence, the machine will remain in the differential mode and the required torque will be achieved using the rated current. Therefore, the current density of the machine will remain the same throughout the wide speed range using all the conditions together. Using PCS, the torque of the machine is not suddenly dropped in differential which was an issue of [22].

To elaborate the effectiveness and limitations of PCS, it is compared with Con3 as shown in Fig. 21. In Con3 only winding switching is used, which is same as [22]. Con3 is analyzed with two types of materials, namely, general and special steel. This is because general steel has high core losses and therefore lower efficiency. Hence, to improve its efficiency, special steel material is used in Con3. In case of Con3 (general steel and special steel), from 0–600 rpm, the machine runs in the cumulative mode. When the inverter limit is reached at 600 rpm, the machine is switched to the differential mode. Moreover, the torque of Con3 is higher than PCS. This is because PCS combines different conditions in a single control strategy to ensure high efficiency during wide speed range operation. Hence, the torque of the machine is low when the machine runs in the Con1 and Con2 configuration.

TABLE 4. Comparison of characteristics of general steel and special steel.

Characteristic	General Steel (50TW470)	Special Steel (20JNHF1300)
Lamination thickness (mm)	0.5	0.2
Saturation limit (Tesla)	1.8	1.5
Eddy current loss coefficient	1.2796	0.05629
Hysteresis loss coefficient	161.28	404.12
Relative permeability at saturation limit	119.36	397.88
Bulk conductivity (Siemens/m)	2000000	1219512

The JNHF-core manufactured by NHF company is a special core with extremely low core losses at high frequencies. For Con3, we re-simulated our machine for wide speed range using a special core. The main characteristics of general steel (Grade:50TW470) and special steel (Grade: 20JNHF1300), as obtained from simulation software 'ANSYS Maxwell', are listed in Table 4.

Special steel has a very low eddy current loss coefficient and low conductivity. Hence, its core losses are very low compared to general steel. Moreover, the lamination thickness of special steel is also small, which further limits the eddy current losses and consequently, results in core losses. However, the demerit of special steel is its lower saturation limit compared to general steel, which increases the phase voltages of the machine.

The torque speed curve and power of Con3 using special steel is also shown in Fig. 21. The torque of the machine is almost same as Con3 (general steel). However, the maximum

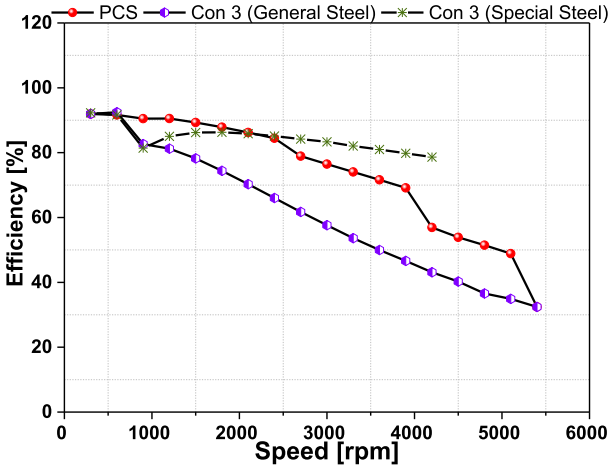

FIGURE 22. Efficiency comparison of proposed control strategy with Con3.

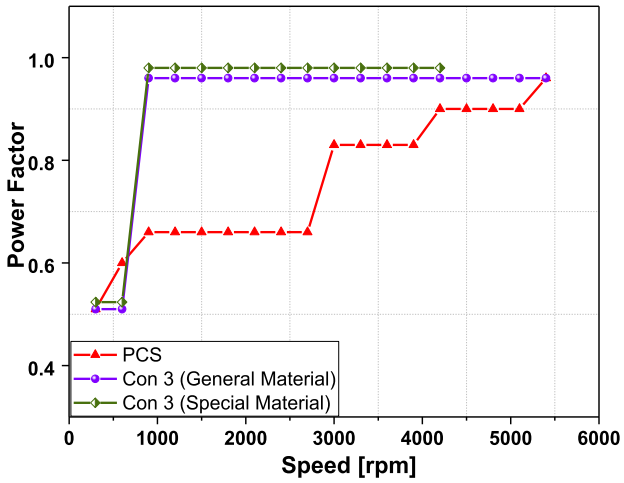

FIGURE 23. Power factor comparison of proposed control strategy with Con3.

speed of the machine is now limited to 4200 rpm. This is because the saturation limit of special steel is lower than that of general steel. The saturation limit of general and special steel is 1.8 T and 1.5 T, respectively. Because all other rated conditions including armature current and turns/phase is same in special and general steel, the machine gets saturated with special steel, which increases the terminal voltages of the machine. Therefore, inverter limit is reached earlier using special steel, which causes the speed limit to be lower compared to that in general steel.

The output power of the PCS is compared with Con3 (general steel and special steel) to show the merits and limitations of PCS. The comparison is shown in Fig. 21. PCS has less output power compared to Con3. This is because the proposed strategy uses less turns and the torque of the machine is thus low. This is a trade off in the proposed technique to get high efficiency during wide speed range. The output power of Con3 (special steel) is almost same to Con3 (general steel) due to their similar output torques. The core losses of the steel can be calculated by Steinmetz equation (10) [25]

$$P_c = P_h + P_e = K_h f B^n + K_e f^2 B^2 \tag{10}$$

where $P_h P_e$, K_h, K_e, f, B are the hysteresis loss, eddy current loss, hysteresis loss coefficient, eddy current loss coefficient, frequency and flux density of the steel respectively.

The efficiency and power factor are the two important characteristics for wide speed range operation. Therefore, the efficiency and power factor of PCS is compared with Con3 (general steel and special steel) as shown in Fig. 22 and Fig. 23, respectively. It can be observed that the PMVM has a much higher efficiency in wide speed range operation using PCS compared to Con3 (general steel). The high efficiency is the main merit of the PCS. Therefore, the proposed control strategy is better for obtaining both a wide speed range and high efficiency.

Moreover, the efficiency of the machine in Con3 with special steel is also shown in Fig. 22. It can be observed that the efficiency of the machine is much higher with special steel. However, the cost of the machine will also be high due to expensive steel. Moreover, the speed of the machine is also limited to 4200 rpm, compared to 5400 rpm of general steel. The reason for limited speed range with special steel was discussed previously.

The power factor comparison of PCS with Con3 (general steel) is also shown in Fig. 23. It can be observed that initially both machines have the same power factor. In Con3 (general steel), the machine is switched to the differential mode at 600 rpm, and its factor is improved to 0.96 in this mode until the maximum speed of 5400 rpm. In PCS, the machine runs in different conditions initially; therefore, the power factor is gradually improved to 0.96. The power factor of the Con3 (special steel) is slightly higher than Con3 (general steel). The same trend can be observed in the cumulative and differential modes of operation with two materials. From the comparison of PCS with Con3 (general and special steel), it can be concluded that the PCS has a better efficiency but a lower power than Con3. Con3 has a higher power when general steel is used but a lower efficiency. However, the efficiency of Con3 can be improved by using special steel. In that case the maximum speed of the machine is lower.

It should be noted however, that the PCS needs two inverters with additional switches, hence, cost of the machine is expected to be high. To avoid failure of additional added switches, secondary fault current and temperature sensor circuits can be installed along with the switches, which will dissipate the fault current as heat or break the circuit to avoid potential damage to the switches. However, utilizing the PCS, the machine achieves better efficiency with same maximum speed limit compared to [22]. Ferrite magnets along with general steel have been used to limit the cost in this analysis. The comparison of efficiency and power of all three control strategies in PMVM is shown in Table 5. The advantages and limitation of all control strategies are shown in Table 6.

TABLE 5. Comparison of all control strategies.

Item (Unit)	Proposed Control Strategy (PCS)	Con 3 (General Steel)	Con 3 (Special Steel)
Efficiency at the base speed (%)	91.9	91.9	94.4
Highest efficiency during wide speed range operation (%)	93.8	92.4	94.4
Lowest efficiency during wide speed range operation (%)	32.4	32.4	80.2
Maximum Power (W)	539	553.8	521.5
Minimum Power (W)	342	526.4	518.3
Maximum Speed (rpm)	5400	5400	4200

TABLE 6. Advantages and disadvantages of all control strategies.

Method	Advantages	Disadvantages
Con1(General Steel)	Good efficiency, same current density throughout wide speed range, low cost	Limited speed range
Con2 (General steel)	Good efficiency, same current density throughout wide speed range, low cost	Speed range better than Con1 but still limited speed range
Con3 (General Steel)	Wide speed range, low cost	Low efficiency, high current density during wide speed range
Con3 (Special steel)	Wide speed range, excellent efficiency	High cost, high current density during wide speed range
PCS (General Steel)	Wide speed range, same current density throughout wide speed range, good efficiency, low cost	Additional switches required

VI. CONCLUSIONS

This paper proposed turn switching along with winding switching for high efficiency during wide speed range operation of PMVMs for electric vehicles application. Further, a control strategy was proposed. Using the proposed control strategy (PCS), the demerits of [22], that are low efficiency in wide speed range and low torque in differential mode are avoided. With low turns for the winding set X, Y, Z (Con1), the machine provided high efficiency during wide speed range operation. However, the maximum speed of the machine was the lowest in this case, that is 3900 rpm. The machine was then investigated using a medium number of turns for winding set X, Y, Z (Con2). In this condition, the maximum speed of the machine was increased to 5100 rpm, however, the efficiency of the machine was found to be lower than Con1. Finally, the machine was analyzed using the same number of turns for winding set A, B, C and X, Y, Z. It was revealed that the machine provides highest power in this condition. Moreover, the maximum speed of the machine was also high compared to Con1 and Con2. However, the machine has lowest efficiency in this mode due to higher core losses. In order to elaborate the advantages and limitations of PCS, it was compared with Con3 (general and special steel). The PCS has better efficiency than Con3 (general steel), however, the power of the machine is low in this case. Moreover, it was revealed that in Con3 (special steel), both the power and efficiency of the machine are high, but the maximum speed of the machine is lower than PCS. Furthermore, the price of the machine will be high due to expensive core material. Therefore, it depends on the end user preference, to use one of the following (1) High power but low efficiency (Con3/general steel) (2) High power and high efficiency with high price (Con3/special steel) (3) Lower power and high efficiency with lower price (proposed control strategy). The experiment of the proposed idea along with further work will be provided in a future research paper.

REFERENCES

[1] X. Sun *et al.*, "Performance analysis of suspension force and torque in an IBPMSM with V-shaped PMs for flywheel batteries," *IEEE Trans. Magn.*, vol. 54, no. 11, Nov. 2018, Art. no. 8105504. doi: 10.1109/TMAG.2018.2827103.

[2] Z. Shi *et al.*, "Torque analysis and dynamic performance improvement of a PMSM for EVs by skew angle optimization," *IEEE Trans. Appl. Supercond.*, vol. 29, no. 2, Mar. 2019, Art. no. 0600305. doi: 10.1109/TASC.2018.2882419.

[3] X. Sun *et al.*, "Performance improvement of torque and suspension force for a novel five-phase BFSPM machine for flywheel energy storage systems," *IEEE Trans. Appl. Supercond.*, vol. 29, no. 2, pp. 1–5, Mar. 2019, Art. no. 0601505. doi: 10.1109/TASC.2019.2893295.

[4] F. Zhao, T. A. Lipo, and B.-I. Kwon, "Dual-stator interior permanent magnet Vernier machine having torque density and power factor improvement," *Electr. Power Compon. Syst.*, vol. 42, pp. 1717–1726, 2014.

[5] B. Kim and T. A. Lipo, "Operation and design principles of a PM Vernier motor," *IEEE Trans. Ind. Appl.*, vol. 50, no. 6, pp. 3656–3663, Nov./Dec. 2014. doi: 10.1109/TIA.2014.2313693.

[6] J. Li, K. T. Chau, J. Z. Jiang, C. Liu, and W. Li, "A new efficient permanent-magnet vernier machine for wind power generation," *IEEE Trans. Magn.*, vol. 46, no. 6, pp. 1475–1478, Jun. 2010.

[7] J. Yang *et al.*, "Quantitative comparison for fractional-slot concentrated-winding configurations of permanent-magnet Vernier machines," *IEEE Trans. Magn.*, vol. 49, no. 7, pp. 3826–3829, Jul. 2013.

[8] T. Zou, D. Li, R. Qu, D. Jiang, and J. Li, "Advanced high torque density PM Vernier machine with multiple working harmonics," *IEEE Trans. Ind. Appl.*, vol. 53, no. 6, pp. 5295–5304, Nov./Dec. 2017.

[9] T. Zou, D. Li, C. Chen, R. Qu, and D. Jiang, "A multiple working harmonic PM Vernier machine with enhanced flux-modulation effect," *IEEE Trans. Magn.*, vol. 54, no. 11, Nov. 2018, Art. no. 8109605.

[10] N. Baloch, B.-I. Kwon, and Y. Gao, "Low-cost high-torque-density dual-stator consequent-pole permanent magnet Vernier machine," *IEEE Trans. Magn.*, vol. 54, no. 11, Nov. 2018, Art. no. 8206105. doi: 10.1109/TMAG.2018.2849082.

[11] X. Ren, D. Li, R. Qu, Z. Yu, and Y. Gao, "Investigation of spoke array permanent magnet Vernier machine with alternate flux bridges," *IEEE Trans. Energy Convers.*, vol. 33, no. 4, pp. 2112–2121, Dec. 2018.

[12] Y. Gao, D. Li, R. Qu, H. Fang, H. Ding, and L. Jing, "Analysis of a novel consequent-pole flux switching permanent magnet machine with flux bridges in stator core," *IEEE Trans. Energy Convers.*, vol. 33, no. 4, pp. 2153–2162, Dec. 2018. doi: 10.1109/TEC.2018.2839727.
[13] Z. Liang, Y. Gao, D. Li, and R. Qu, "Design of a novel dual flux modulation machine with consequent-pole spoke-array permanent magnets in both stator and rotor," *CES Trans. Elect. Mach. Syst.*, vol. 2, no. 1, pp. 73–81, Mar. 2018. doi: 10.23919/TEMS.2018.8326453.
[14] F. Zhao, T. A. Lipo, and B.-I. Kwon, "A novel dual-stator axial-flux spoke-type permanent magnet Vernier machine for direct-drive applications," *IEEE Trans. Magn.*, vol. 50, no. 11, Nov. 2014, Art. no. 8104304. doi: 10.1109/TMAG.2014.2329861.
[15] B. Kim and T. A. Lipo, "Analysis of a PM Vernier motor with spoke structure," *IEEE Trans. Ind. Appl.*, vol. 52, no. 1, pp. 217–225, Jan./Feb. 2016. doi: 10.1109/TIA.2015.2477798.
[16] D. Li, R. Qu, and T. A. Lipo, "High-power-factor Vernier permanent-magnet machines," *IEEE Trans. Ind. Appl.*, vol. 50, no. 6, pp. 3664–3674, Nov./Dec. 2014. doi: 10.1109/TIA.2014.2315443.
[17] L. Wu, R. Qu, D. Li, and Y. Gao, "Influence of pole ratio and winding pole numbers on performance and optimal design parameters of surface permanent-magnet Vernier machines," *IEEE Trans. Ind. Appl.*, vol. 51, no. 5, pp. 3707–3715, Sep./Oct. 2015. doi: 10.1109/TIA.2015.2426148.
[18] N. Baloch, S. Khaliq, and B.-I. Kwon, "HTS dual-stator spoke-type linear Vernier machine for leakage flux reduction," *IEEE Trans. Magn.*, vol. 53, no. 11, Nov. 2017, Art. no. 8111104. doi: 10.1109/TMAG.2017.2699641.
[19] C. Liu, J. Zhong, and K. T. Chau, "A Novel flux-controllable Vernier permanent-magnet machine," *IEEE Trans. Magn.*, vol. 47, no. 10, pp. 4238–4241, Oct. 2011. doi: 10.1109/TMAG.2011.2152374.
[20] H. Wang *et al.*, "A novel consequent-pole hybrid excited Vernier machine," *IEEE Trans. Magn.*, vol. 53, no. 11, Nov. 2017, Art. no. 8112304. doi: 10.1109/TMAG.2017.2695494.
[21] H. yang, H. Lin, Z.-Q. Zhu, S. Fang, and Y. Huang, "A dual-consequent-pole vernier memory machine," *Energies*, vol. 9, no. 3, p. 134, 2016. doi: 10.3390/en9030134.
[22] A. Arif, N. Baloch, and B.-I. Kwon, "Wide speed range operation of permanent magnet Vernier machines," *Electron. Lett.*, vol. 54, no. 18, pp. 1070–1072, Sep. 2018. doi: 10.1049/el.2018.5008.
[23] S. Atiq, T. A. Lipo, and B.-I. Kwon, "Wide speed range operation of non-salient PM machines," *IEEE Trans. Energy Convers.*, vol. 31, no. 3, pp. 1179–1191, Sep. 2016. doi: 10.1109/TEC.2016.2547421.
[24] X. Sun, Y. Shen, S. Wang, G. Lei, Z. Yang, and S. Han, "Core losses analysis of a novel 16/10 segmented rotor switched reluctance BSG motor for HEVs using nonlinear lumped parameter equivalent circuit model," *IEEE/ASME Trans. Mechatronics*, vol. 23, no. 2, pp. 747–757, Apr. 2018. doi: 10.1109/TMECH.2018.2803148.
[25] G. Bertotti, *Hysteresis in Magnetism: For Physicists, Materials Scientists, and Engineers*. Waltham, MA, USA: Academic.

ARSALAN ARIF was born in 1984. He received the B.S. degree in electrical engineering from the University of Engineering and Technology (UET), Peshawar, Pakistan, in 2006, and the M.S. degree in electronics system engineering from Hanyang University, Ansan, South Korea, in 2010, where he is currently pursuing the Ph.D. degree with the Department of Electronics System Engineering. From 2010 to 2013, he was a Lecturer with the Sarhad University of Science and Information Technology (SUIT), Pakistan. His research interest includes design and control of electrical machines.

NOMAN BALOCH was born in 1987. He received the B.S. degree in electronics engineering from the Balochistan University of Information Technology, Engineering and Management Sciences (BUITEMS), Quetta, Pakistan, in 2010. He is currently pursuing the M.S. and Ph.D. degrees with the Department of Electronics System Engineering, Hanyang University, Ansan, South Korea.

From 2010 to 2015, he was the Deputy Assistant Director of the National Database and Registration Authority (NADRA), Pakistan. His research interest includes design and control of electrical machines.

BYUNG-IL KWON was born in 1956. He received the B.S. and M.S. degrees in electrical engineering from Hanyang University, Ansan, South Korea, in 1981 and 1983, respectively, and the Ph.D. degree in electrical engineering, machine analysis from the University of Tokyo, Tokyo, Japan, in 1989. From 1989 to 2000, he was a Visiting Researcher with the Faculty of Science and Engineering Laboratory, University of Waseda, Tokyo. In 1990, he was a Researcher with the Toshiba System Laboratory, Yokohama, Japan. In 1991, he was a Senior Researcher with the Institute of Machinery and Materials Magnetic Train Business, Daejeon, South Korea. From 2001 to 2008, he was a Visiting Professor with the University of Wisconsin–Madison, Madison, WI, USA. He is currently a Professor with Hanyang University. His research interest includes design and control of electrical machines.